CrossMark

Performance Based Evaluation of Carbonation Resistance of Concrete According to Various Curing Conditions from Climate Change Effect

Tae-Kyun Kim[1] , Seung-Jai Choi[1], Jang-Ho Jay Kim[1],* , Yong-Sik Chu[2], and Eunjong Yu[3]

Abstract: Recently, extreme climate change has been occurring globally not only in the simple form of temperature increases but also in a wide range of extreme climatic events, such as abnormal drought conditions and frequent typhoons. Among these various events, the greatest problem is found in global warming. The earth's temperature has risen since the period of rapid industrial growth in the 1970s, and global warming occurs at the local level of regions and cities as well as the national level. The greenhouse gases that influence global warming include various types of chemical components, such as carbon dioxide (CO_2), perfluorocarbons (PFCs), nitrous oxide (N_2O), and methane (CH_4). In addition, climate change is extending the construction period of concrete structures. Whereby increasing related economic losses. Pushing through construction projects without considering climate change is leading to concrete quality deterioration, causing poor constructions and consequently resulting in humans casualties and property damage. In particular, atmospheric CO_2 generates calcium carbonate by reacting with concrete hydration products. This result is reinforcing bar corrosion and concrete durability reduction due to lowered alkalinity. Therefore, in this study, concrete durability performance with respect to carbonation resistance from curing conditions change due to wind speed and sunlight exposure time is evaluated. Based on concrete carbonation resistance data obtained using curing conditions of various wind speed and sunlight exposure time, performance based evaluation (PBE) is performed using the satisfaction curve (SC) developed from the carbonation resistance test results. Using the developed PBE of concrete performance, future concrete performance is predicted based on future climate scenario. Also, the concrete mix design solutions to the concrete performance degradation due to climate change effect is proposed.

Keywords: satisfaction curve, performance based evaluation, concrete, carbonation resistance, climate change.

1. Introduction

Extreme climate change takes the form of geographically diverse environmental conditions. The causes of climate change can largely be divided into natural factors and human factors. Natural factors include the increase in aerosol due to solar activity, solar radiation, and volcanic eruptions, while human factors include the excessive use of fossil fuels and deforestation (Kang 2004). The various consequences of climate change include extreme climatic events such as super typhoons, extreme snowfall, and heat waves, and in fact, the frequency of such events is rising rapidly globally. Therefore,

construction technology and standards to respond to the climate change that is currently occurring are urgently needed. In addition, the Earth's temperature has risen since the period of rapid industrial growth in the 1970s. This climate change has caused a variety of problems, the most serious of which is the increase in the average temperature due to global warming. Moreover, the greenhouse gases that influence global warming include various types of chemical components, such as CO_2, PFCs, N_2O, and CH_4 (Pachauri and Meyer 2014; Stoker et al. 2013). In particular, among the greenhouse gases, CO_2 accounts for approximately 90%, and it can have a significant impact on reinforced concrete. As a construction material, concrete has exceptional durability performance, and it accounts for over 70% of constructional materials used in building infrastructures. However, concrete curing performance may decrease due to physical and chemical factors depending on the exposed environment. In particular, atmospheric CO_2 generates calcium carbonate by reacting with concrete hydration products. This results in the corrosion of reinforcing bars and reduced concrete durability due to lowered alkalinity (Chang and Chen 2006; Lo and Lee 2002; Fattuhi 1988; Al-Khaiat and Fattuhi 2002). As concrete carbonation occurs slowly in a long term in terms of reaction rate, a great deal of time and effort are required for measurement (Kim et al. 2008; Kwon et al. 2007; Jung and Kim 2010). Therefore, in this

[1]School of Civil and Environmental Engineering, Yonsei University, 134 Shinchon-dong, Seodaemun-gu, Seoul 03722, South Korea.
*Corresponding Author; E-mail: jjhkim@yonsei.ac.kr
[2]KICET, Soho-ro, Jinju-si, Gyeongsangnam-do, Seoul 52851, South Korea.
[3]Department of Architectural Engineering, Hangyang University, 222 Wangsipri-ro, Sungdong-gu, Seoul 04763, South Korea.

study, concrete durability performance with respect to carbonation resistance from curing conditions change due to wind speed and sunlight exposure time. Concrete carbonation resistance experiments are performed. Using wind speed and sunlight exposure time. Also, performance based evaluation (PBE) through the satisfaction curve (SC) based on the carbonation resistance test results are performed. In addition, PBE will be conducted along with future climate scenario for 2050, and comparative analysis with past data.

2. Performance Based Evaluation

The PBE used in this study creates a SC using the Bayesian probability method (Phan et al. 2012; Kim et al. 2011 2012), which uses information obtained from sampling, and uses no other information than that obtained from sampling when making a statistical inference. In addition, the method for decision-making based on the information obtained statistically in an uncertain situation, as used in this study, is based (and sometimes relies) on the Bayesian probability method. For example, based on the experimental data obtained on wind speed and sunlight exposure time as concrete curing conditions, for which existing studies are lacking, this study predicts durability performance using Bayesian probability. When durability performance is verified using this method, casualties and property damages can be prevented.

According to the Bayesian theorem (Ang and Tang 1984; Box and Tiao 1973), if Event A occurrs and is classified into Group B in the past, when the same Event A occurs in the future, it is likely to be placed in Group B.

$$P(Wi|A) = P(A|Wi)P(Wi)/P(A) \tag{1}$$

Equation (1) represents posterior probability. As described above, $P(Wi|A)$ is the probability of an individual incident belonging to Wi when the individual incident has Trait A. When it is assumed that a total group of incidents is divided into two groups of incidents, W1 and W2, the following equation is established.

$$P(W1|A) + P(W2|A) = 1 \tag{2}$$

This is because an individual incident certainly belongs to either W1 or W2. When it is assumed that $P(W1|A) = 0.7$ and $P(W2|A) = 0.3$ based on existing data, and a new individual incident with Trait A is encountered in the future, A can be classified as W1. Accordingly, when an individual incident has Trait A, it is predicted that A would belong to the Wi with the largest $P(Wi|A)$ value. When it is assumed that $P(W1|A) < P(W2|A)$, it can be predicted that A belongs to Group W2. Replacing both the right and left sides using Eq. (1) results in

$$P(A|W1)P(W1)/P(A) < P(A|W2)P(W2)/P(A) \tag{3}$$

Equation (3) can be summarized as Eq. (4).

$$P(A|W1)/P(A|W2) < P(W2)/P(W1) \tag{4}$$

Equation (4) represents the Bayesian theorem. When a known individual incident has Trait A, the individual incident can be determined whether it belongs to W1 or W2 using Eq. (4) based on which side of the equation is larger; that is, the individual belongs to W1 if the left side of Eq. (4) is larger and W2 if the right side is larger. The left side of Eq. (4) is the likelihood ratio and the right side is the threshold where both values can be obtained from past experiences. In conclusion, a group of incidents is determined depending on whether the likelihood ratio exceeds the threshold.

In addition, the PBE method conducts evaluation using a SC, and is similar to the Fragility curve that utilizes Bayesian method and is used in seismic performance evaluation (Ang and Tang 1984; Box and Tiao 1973). Shinozuka proposed the concept of the fragility curve using Bayesian statistical method in evaluating vulnerability of a structure to earthquake (Shinozuka et al. 2000, 2001; Singhal and Kiremidjian 1988, 1996).

The fragility method developed by Shinozuka and Singhal uses a fragility curve in evaluating the vulnerability of a bridge or a structure probabilistically, and represents conditional probabilities of an excess property in relation to a limit target, such as a collapse of a structure in relation to ground vibration intensity, using a normal distribution function curve. Means and log standard deviations are estimated using the maximum likelihood estimation equation shown in Eq. (5).

$$L = \prod_{i=1}^{N} [F(a_i)]^{x_i} [1 - F(a_i)]^{1-x_i} \tag{5}$$

Here, $F(.)$ denotes the fragility curve at a specific damage stage, a_i denotes the value of Peak Ground Acceleration (PGA) for the bridge, i and x_i is determined as 0 or 1 according to the damage to the bridge below the PGA value ai and N is determined as the total number of bridges surveyed after an earthquake. Under the assumptions of the commonly used log normal distribution, $F(a)$ can take the form as shown in Eq. (6).

$$F(a) = \Phi\left[\frac{\ln\left(\frac{a}{c}\right)}{\xi}\right] \tag{6}$$

Here, a denotes PGA and $\Phi[.]$ denotes standardized normal distribution function. In Eq. (6), c and ξ are the values obtained to maximize $\ln L$, which is expressed as Eq. (7).

$$\frac{d \ln L}{dc} = \frac{d \ln L}{d\xi} = 0 \tag{7}$$

Since SC is a statistical method to determine the success or failure of a chosen variable using the satisfaction ratio between 0.0 and 1.0, a large number of data are required. However, experimental data required for creating a SC are usually insufficient. In order to overcome this limitation, a normal distribution curve is generated using actual experimental data. Then, virtual data are derived from the curve.

The virtual data generation method that is used for this study is explained in detail in a publication on SC development method (Kim et al. 2012).

This study aims to determine the changes in material properties of concrete due to climate change using the PBE method by generating SC that represent the changes in wind speed and sunlight exposure time, as climate change factors that can have greatest impacts on material properties of concrete.

3. Experimental Details

3.1 Mixture Conditions
The concrete mixing table used in this study is shown in Table 1, and the mixing design was the maximum size of coarse aggregate at 25 mm, water–cement ratio at 55%, slump at 120 ± 2 mm, and 28-day target design strength at 27 MPa. Regarding concrete specimens for compressive strength experiment and slump experiment, 100×200 mm cylinder specimens were created based on KS F 2403 [KS F 2403].

3.2 Curing Conditions
Tables 2 and 3 show monthly averages of wind speed and sunlight exposure time for Seoul over the past 10 years [http://www.kma.go.kr/]. The wind speed data show that most annual and monthly averages are between 2 and 3 m/s, and the sunlight exposure time data also show that annual and monthly averages are similar to one another as in the case of wind speed data. However, the data show that monthly averages of sunlight exposure time for July and August are markedly lower than those of other months. This indicates that sunlight exposure time is different from the amount of sunshine. Sunlight exposure time refers to the amount of time sunlight illuminates the Earth's surface, and in July and August, due to the rainy season and typhoons, the actual amount of time that the sunlight illuminates the Earth's surface decreases. Therefore, in this study, considering these facts, wind speed was set at 0, 2, 4, and 6 m/s, and sunlight exposure time values were set at 2, 4, 6, and 8 h as shown in Table 4. Then, experiments were conducted using various combinations of the conditions.

3.3 Carbonation Resistance Test
Wind speed and sunlight exposure time curing shown in Table 4 was conducted for 28-days, and then, the specimens were moved to carbonation test equipment as shown in Fig. 1, where an additional 28-days curing was conducted.

Carbonation test was conducted at 20 ± 2 °C temperature, and 95% or higher relative humidity, and $5 \pm 0.2\%$ CO_2, based on KS F 2584 [KS F 2584]. For carbonation test, square mold specimen and circular specimen were used. Square mold specimens are cross-sectionally square (100 mm in length of one side), and the length of specimen is 400 mm. For the purpose of a single measurement, a circular specimen sized 100 mm $\times$ 200 mm or 150 mm $\times$ 300 mm is created and used. In this study, due to the purpose of a single measurement, 100 mm $\times$ 200 mm circular specimens were used, and for each case, three specimens were created. The measurement of carbonation depth was conducted by breaking up the splitting surface of the specimen. The reagent used in the carbonation was produced in a solution to use in the experiment based on the production process specified in KS M 8238. Phenolphthalein solution specified in KS M 8238 was used as indicator, and the solution was produced by melting phenolphthalein powder 1 g in 95% ethanol 90 mL and adding water to make it 100 mL. However, if the specimen is very dry, it can be made with 95% ethanol 70 mL and more water added. In this study, as curing humidity was set at 95% or higher, reagent was produced with ethanol 90 mL. Measurement period of carbonation depth is usually conducted in 1, 4, 8, 13, or 26 weeks, and in this study measurement was conducted at the fourth week by considering curing period.

3.4 Carbonation Resistance Measurement
The method for carbonation depth measurement includes obtaining 10 data points from two sides of each specimen, which totals 30 points from six sides from three specimens for each case, and then obtaining the mean of carbonation depth for each case and rounding it up to the nearest 0.5 mm. When spraying phenolphthalein solution on the cross-sectionally cut surface of carbonated specimen, the part that has not been carbonated turns purple in color. Carbonation progresses from outside to inside, and the length between concrete surface and the boundary of non-carbonated part is called carbonation depth. The common equation to obtain carbonation rate modulus (constant), A, is shown in Eq. (8), and constant Ct can be obtained from experiment results.

$$C_t = A\sqrt{t}$$
$$A = \frac{C_t}{\sqrt{t}} \tag{8}$$

Here, A denotes carbonation rate modulus, Ct denotes carbonation depth (mm), and t denotes carbonation period (week).

Table 1 Mix proportion of concrete.

Coarse aggregate size (mm)	W/C (%)	Unit (kg/m³)				f_{ck} (MPa)
		W	C	S	G	
25	55	183	333	677	1014	27

W water, *C* cement, *S* fine aggregate, *G* coarse aggregate, f_{ck} design criterion strength.

Table 2 Monthly mean wind speed at Seoul, Korea (0.1 m/s).

Year	Jan.	Feb.	Mar.	Apr.	May.	Jun.	Jul.	Aug.	Sep.	Oct.	Nov.	Dec.	Avg.
2012	25	29	35	34	27	28	27	30	23	23	27	27	27.92
2011	28	26	34	32	28	29	24	25	24	21	27	26	27.00
2010	23	24	29	29	26	21	25	24	23	22	28	30	25.33
2009	25	25	31	26	25	25	23	22	18	21	25	25	24.25
2008	23	27	26	27	27	27	24	25	19	20	22	25	24.33
2007	20	23	27	28	26	23	24	26	25	21	22	24	24.08
2006	21	26	29	30	25	22	23	21	21	20	24	21	23.58
2005	24	28	29	30	24	24	22	26	23	17	22	25	24.50
2004	21	29	27	27	26	21	23	24	22	20	20	22	23.50
2003	25	22	23	25	18	20	18	14	11	20	20	24	20.00
2002	23	20	21	23	23	20	21	20	16	20	24	22	21.08
Avg.	23.45	25.36	28.27	28.27	25.00	23.64	23.09	23.36	20.45	20.45	23.73	24.64	24.14

KMA Korea Meteorological Administration.

Table 3 Monthly mean sunlight exposure time at Seoul, Korea.

Year	Jan.	Feb.	Mar.	Apr.	May.	Jun.	Jul.	Aug.	Sep.	Oct.	Nov.	Dec.	Avg.
2012	6.15	7.76	6.19	7.08	8.11	7.73	4.65	5.12	6.36	7.59	6.04	6.25	6.58
2011	7.05	5.95	7.75	6.74	5.82	5.69	2.59	3.03	6.01	6.95	4.32	6.31	5.68
2010	5.42	5.04	4.29	5.54	5.76	6.77	2.90	3.11	4.88	6.28	6.01	5.09	5.09
2009	6.79	4.49	6.54	6.82	7.75	6.03	3.74	4.87	6.72	7.62	4.34	4.71	5.87
2008	5.37	7.73	6.04	6.94	6.90	5.79	2.54	6.34	6.15	5.97	5.66	5.06	5.87
2007	5.87	6.13	4.75	6.39	6.36	5.84	2.95	3.41	2.84	5.51	6.28	4.54	5.07
2006	5.20	6.16	6.51	4.53	6.42	5.19	1.11	5.71	6.52	5.97	5.12	5.14	5.30
2005	6.18	6.35	7.16	6.65	7.59	'4.61	2.56	3.33	3.79	6.45	5.75	6.58	5.58
2004	5.69	6.42	7.15	7.01	5.38	5.05	2.75	4.77	5.61	8.15	5.22	6.23	5.79
2003	2.98	3.39	3.36	4.19	5.51	3.39	2.79	2.68	3.35	6.31	3.80	5.81	3.96
2002	3.24	3.71	4.15	5.75	5.65	5.43	2.71	1.69	3.98	4.73	3.15	2.61	3.90
Avg.	5.45	5.74	5.81	6.15	6.48	5.59	2.84	4.01	5.11	6.50	5.06	5.30	5.34

KMA Korea Meteorological Administration.

Table 4 Wind speed and sunlight exposure time curing condition combinations.

Case	Wind speed (m/s)	Sunlight exposure time (h)	Case	Wind speed (m/s)	Sunlight exposure time (h)
1	0	2	9	4	2
2	0	4	10	4	4
3	0	6	11	4	6
4	0	8	12	4	8
5	2	2	13	6	2
6	2	4	14	6	4
7	2	6	15	6	6
8	2	8	16	6	8

Fig. 1 Concrete carbonation chamber.

4. Experimental Results

4.1 Concrete Strength Results

Table 5 shows compressive strengths and splitting tensile strengths of specimen cured at various wind speed and sunlight exposure time levels. The changes in compressive strength show that 28-day compressive strength decrease to approximately 40% of the target design strength of 27 MPa in wind-speed conditions of 2, 4, and 6 m/s (except 0 m/s) for all specimens. In relative strength comparison, the trend of compressive strength showed reduction as the wind speed increased, and vice versa. However, there was an exception in which compressive strength was slightly greater at 6 m/s than at 2 m/s of wind speed. Also, this discrepancy in strength was observed when the sunlight exposure time was longer. More specifically, for the cases of sunlight exposure time 6–8 h (cases 3–4 and 7–8) and 4–6 h (cases 14 and 15), the strength slightly decreased as the sunlight exposure time increased. The examinations of the out of the ordinary

Table 5 Strength test results of wind speed—sunlight exposure time.

Case	Wind speed (m/s)	Sunlight exposure time (h)	Compressive strength (MPa)			Splitting tensile strength (MPa)		
			3 days	7 days	28 days	3 days	7 days	28 days
1	0	2	15.57	24.24	25.94	1.45	1.92	2.12
2	0	4	14.28	23.78	28.18	1.4	1.9	2.22
3	0	6	15.49	23.55	29.36	1.39	1.9	2.4
4	0	8	15.99	22.87	28.46	1.52	1.95	2.05
5	2	2	14.66	19.34	17.55	1.3	2.2	2.07
6	2	4	12.51	18.17	16.44	1.6	1.94	1.65
7	2	6	14.34	22.25	18.36	1.48	2.05	2.02
8	2	8	16.45	22.87	17	1.59	2.17	1.93
9	4	2	14.66	18.97	15.21	1.6	1.98	2.17
10	4	4	13.7	21.01	16.08	1.68	1.99	2.02
11	4	6	14.27	21.8	16.57	1.7	2.14	1.83
12	4	8	13.33	19.91	19.48	1.46	2.21	1.71
13	6	2	15.11	22.1	17.62	1.74	2.16	1.95
14	6	4	13.03	21.65	20.4	1.6	2.18	1.78
15	6	6	14.46	22.66	19.29	1.61	2.05	2
16	6	8	13.18	19.65	21	1.33	2.23	1.7
Control specimens								
Thermo-hydrostatic curing	0	0	17.06	23	31.11	1.58	2.18	2.25
Wet curing	0	0	18.24	26.6	38.32	1.72	2.29	2.7
Air dry curing	0	0	16.13	23.36	28.61	1.36	1.84	2.2

results revealed that they occurred because the average compressive strength values from only three specimens for each test case were used for the evaluation. It is safe assume that if more specimens are used then, the trend will be similar to the expected trend.

Also, the reason for the lower strengths in the wind speed conditions is presumably that when concrete is subjected to continuous wind during the curing process where hydration reaction occurs, the moisture within concrete moves and evaporates in the direction of wind, which interferes with sufficient hydration reaction, and over time, leads to reduced strength. In actual construction sites, such curing conditions are also likely to cause cracks and result in quality deterioration. On the other hand, it was found that the strength of concrete cured at 0 m/s wind speed did not decrease, and 28-day strength was higher at longer sunlight exposure times.

4.2 Concrete Carbonation Depth and Rate Modulus

Tables 6 and 7 tabulate carbonation depth and rate modulus for wind speed (0, 2, 4, and 6 m/s) and sunlight exposure time (2, 4, 6, and 8 h), respectively. The tables showed that maximum and minimum carbonation depth of 8.9 mm and 5.2 mm, respectively, occurred under the wind speed and sunlight exposure time curing conditions of 6 m/s and 8 h and 0 m/s and 2 h, respectively. From Table 6, the curing conditions of 6 m/s and 6 h gives a higher carbonation depth result of 9.1 mm. Also, the maximum and minimum carbonation rate modulus of 4.46 and 2.62, respectively, occurred under the wind speed and sunlight exposure time curing conditions of 6 m/s and 8 h and 0 m/s and 2 h, respectively. Looking at Table 7, the curing

conditions of 6 m/s and 6 h gives a higher carbonation rate modulus result of 4.53 mm. However, this value is an irregular data due to an out of ordinary conditions. One hypothesis that can be associated with this exception is that the calculation of an average depth value was from only three tested specimens for each test case, which would not reflect the proper result. Figures 2 and 3 show the data in Tables 6 and 7 as bar graph for comparison. As shown in Fig. 2a, the carbonation depth results from wind speed curing condition variation shows that the depth increases from 0 to 4 m/s, while, the depth remains unchanged from 4 to 6 m/s. With respect to the depth from sunlight exposure time curing condition variation, shown in Fig. 2b, the depth increases at a same rate for the wind speed variations of 0 - 4 m/s under a constant sunlight exposure time of 2, 4, 6, and 8 h.

As shown in Fig. 3a, the carbonation rate modulus results from wind speed curing condition variation shows that the depth increases from 0 to 4 m/s. However, the rate modulus remains unchanged from 4 to 6 m/s. With respect to the rate modulus from sunlight exposure time curing condition variation shown in Fig. 3b, the rate modulus increases at a same rate for the wind speed variations of 0–4 m/s under a constant sunlight exposure time of 2, 4, 6, and 8 h.

Moreover, the carbonation depth and rate modulus obtained from the specimens cured under thermo-hydrostatic and wet curing conditions were approximately 10% of those specimens from the cured under various wind speed and sunlight exposure time. Also, the carbonation depth and rate modulus of the air cured specimens equivalent to a general environmental conditions were approximately 40% of those from the various curing conditions specimens, with similar trends in the carbonation depth and rate modulus results. In

**Table 6** Test results of concrete carbonation depth (unit: mm).

Wind speed	Sunlight exposure time			
	2	4	6	8
0	5.2	6.4	6.5	6.9
2	6.4	7.0	7.7	7.9
4	8.3	8.5	8.6	8.6
6	8.6	8.5	9.1	8.9

* Thermo-hydrostatic curing: 0.8, ** wet curing: 0.6, *** air dry curing: 4.9.

Table 7 Test results of concrete carbonation rate modulus (unit: $mm/\sqrt{weeks}$).

Wind speed	Sunlight exposure time			
	2	4	6	8
0	2.62	3.18	3.27	3.46
2	3.21	3.49	3.84	3.93
4	4.17	4.23	4.29	4.30
6	4.28	4.24	4.53	4.46

* Thermo-hydrostatic curing: 0.38, ** wet curing: 0.28, *** air dry curing: 2.47.
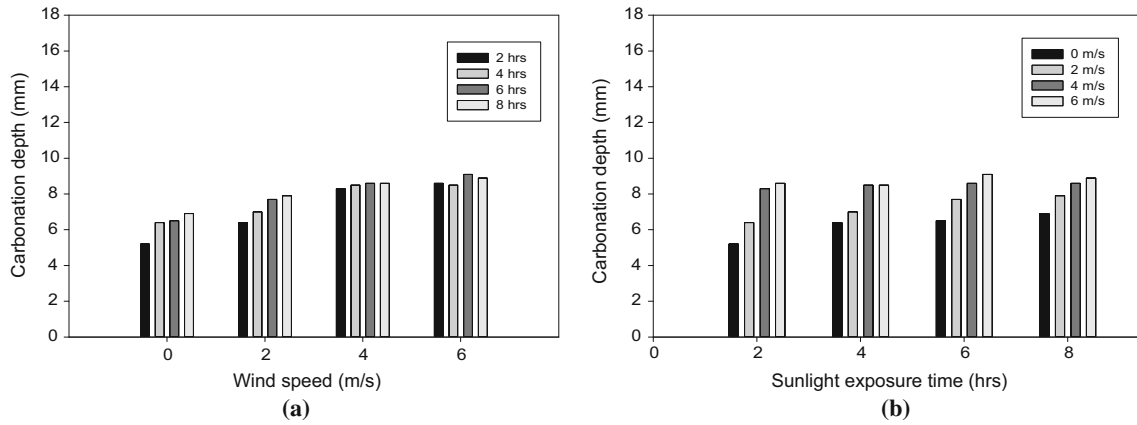
Fig. 2 Carbonation depth versus wind speed and sunlight exposure time. **a** Wind speed with 0, 2, 4, 6 m/s. **b** Sunlight exposure time with 2, 4, 6, 8 h.
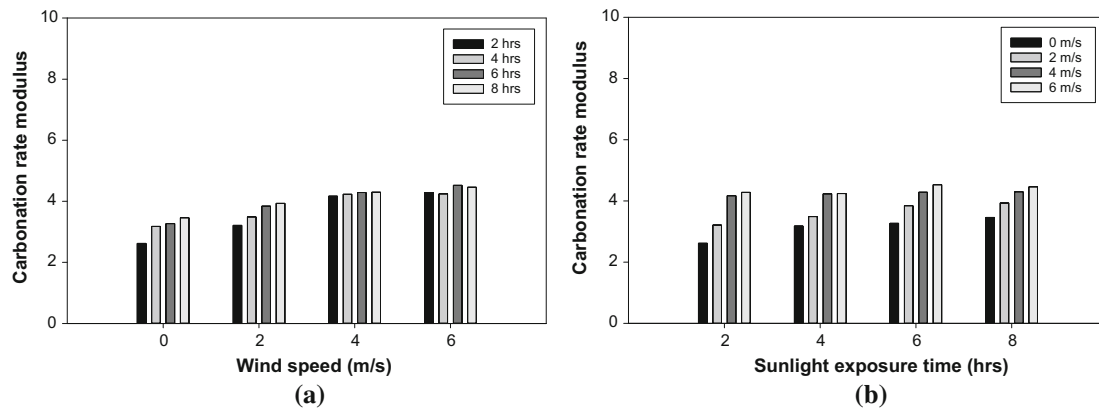
Fig. 3 Carbonation rate modulus versus wind speed and sunlight exposure time. **a** Wind speed with 0, 2, 4, 6 m/s. **b** Sunlight exposure time with 2, 4, 6, 8 h.

conclusion, the carbonation depth increased as the wind speed and sunlight-exposure time increased. The results demonstrated that carbonation rate modulus decreases as relative humidity increases in the curing process, which can be associated with in climate conditions of greater wind speed and sunlight-exposure time. From these harsher climate conditions, curing becomes increasingly difficult and porosity in specimens increase, making it easier for carbon dioxide to penetrate faster and deeper. The results suggest that climate factors play a major role in concrete carbonation resistance.

5. Satisfaction Curve

5.1 Satisfaction Curve of Carbonation Depth

Figures 4, 5, 6, 7, 8, 9, 10, and 11 show the SCs on carbonation depth and carbonation speed modulus as functions of wind speed and sunlight exposure time. After determining the success/failure statuses of experimental data and ascribing them values of 0 and 1 based on whether they meet designer's criteria, the mean and standard deviation can be obtained using the Bayesian probability program, and SCs can be generated based on them. To create the SCs, required satisfaction criteria must be designated. In this

study, the criteria that are applicable to actual construction sites were established. Casting was conducted in the room with no direct contact with outside air or soil, and reinforcing bars of D 35 or less were used, and the thickness of concrete covering was assumed to be 20 mm. As a method to evaluate carbonation durability evaluation of concrete structure, the predicted carbonation depth value, (mm), can be obtained using Eq. (9).

$$\gamma_p y_p \leq \varphi_k y_{lim} \tag{9}$$

Here, γ_p denotes environment coefficient for carbonation, 1.1; ϕ_k denotes durability reduction factor for carbonation, which is generally 0.92; and y_{lim} denotes carbonation limit depth (mm) where reinforcing bars may be corroded, which can be calculated using Eq. (10).
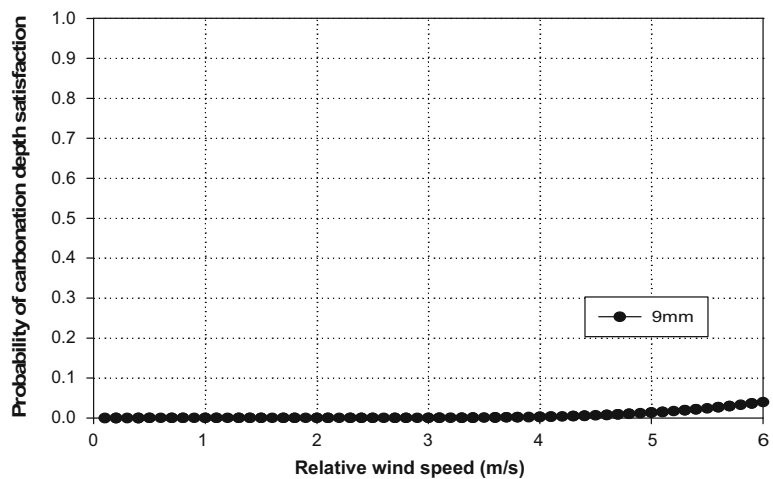
$$y_{lim} = c - c_k \tag{10}$$

In the equation, c denotes design cover thickness (mm), c_k denotes the margin of limit carbonation depth, which is set at 10 mm for natural environment, and 25 mm for severe carbonation attack environment. In this study, as cover thickness was set at 20 mm, the predicted carbonation depth value is about 8.36 mm.
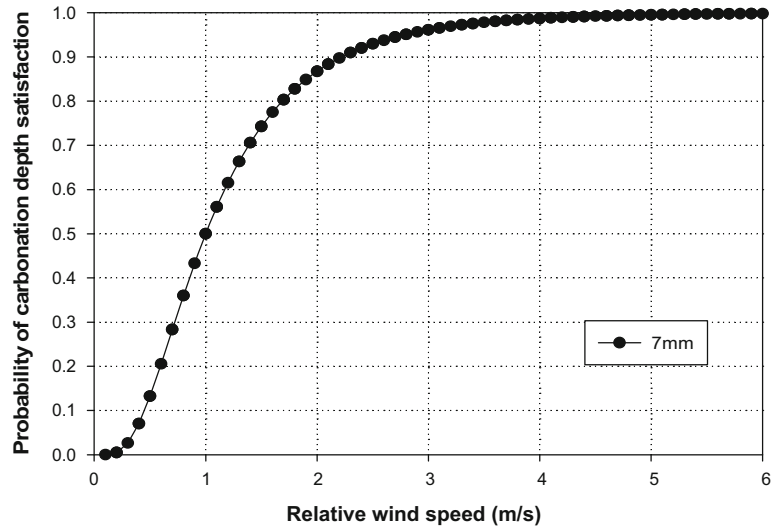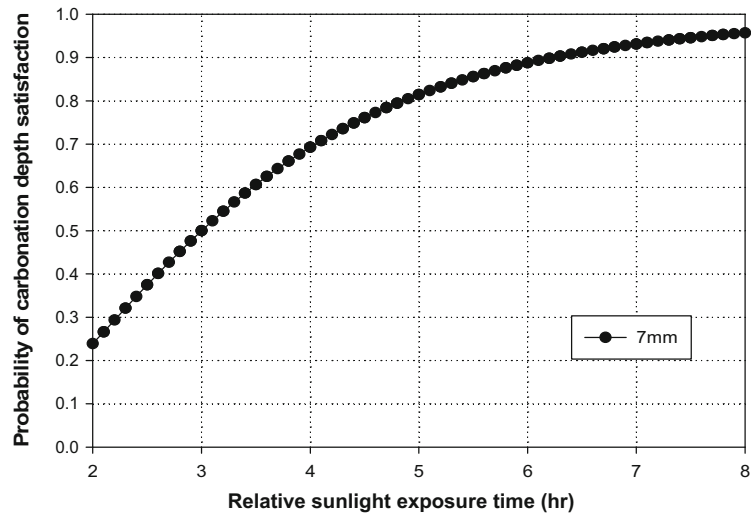
(a)
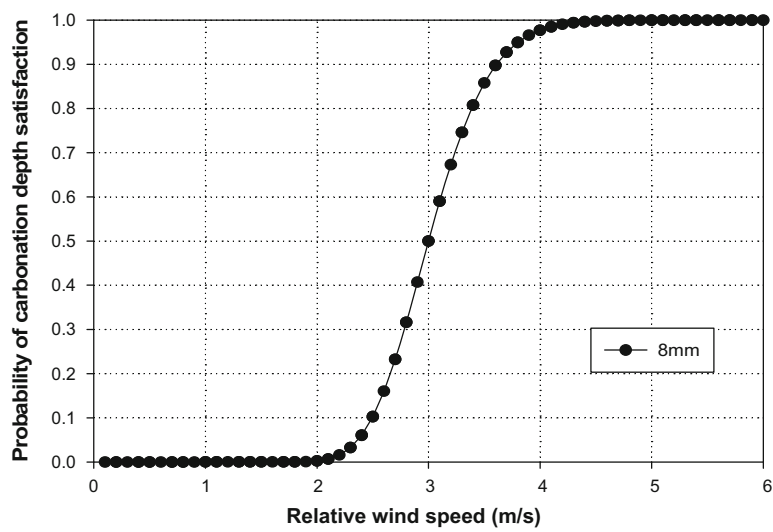
(b)

(c)

Fig. 4 Satisfaction curve of wind speed parameter for carbonation depth. **a** 7 mm, **b** 8 mm, **c** 9 mm

Accordingly, required satisfaction specification was set at 8 mm, and to comparatively analyze various satisfaction probabilities, 7 and 9 mm were added to the satisfaction specification.

Graphs in Figs. 4, 5, 6, 7 show SCs on carbonation depth, where satisfaction specification of 7, 8, and 9 mm was applied. The graphs show that to evaluate the SCs, for example, in the case of Fig. 6, when wind speed-based
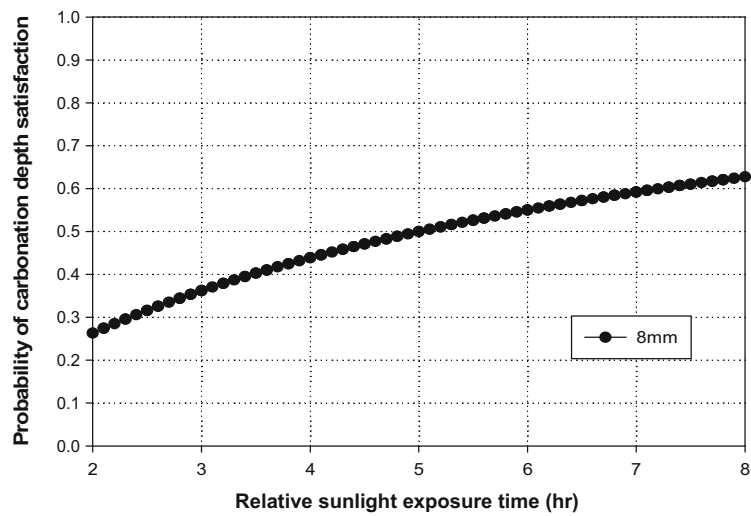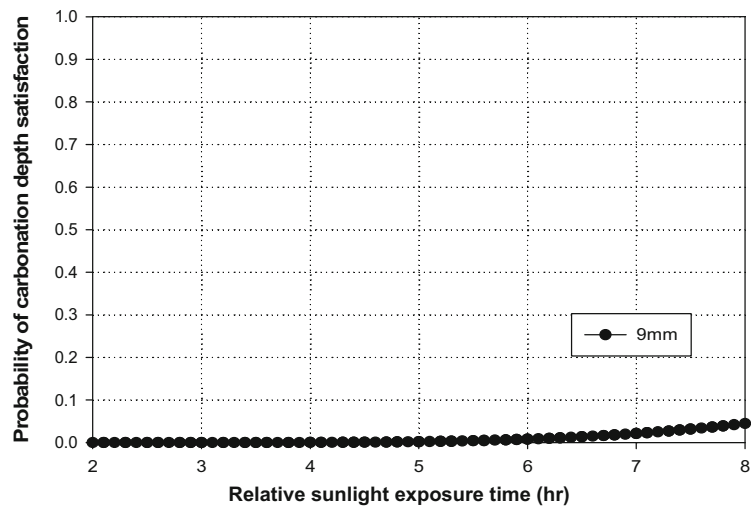
Fig. 5 Satisfaction curve of sunlight exposure time parameter for carbonation depth. **a** 7 mm, **b** 8 mm, **c** 9 mm

carbonation depth criterion is set at 8 mm, to satisfy 50% probability, wind speed must be at least 3 m/s during curing; when the criterion is set at 7 mm, wind speed must be at least 1 m/s. It is also shown that, in the case of Fig. 7, when

carbonation depth criterion is set at 7 mm, to show at least 80% satisfaction probability, 5 h of curing sunlight exposure time should be provided. In the case of carbonation depth, it was found that SC range is larger in wind speed than
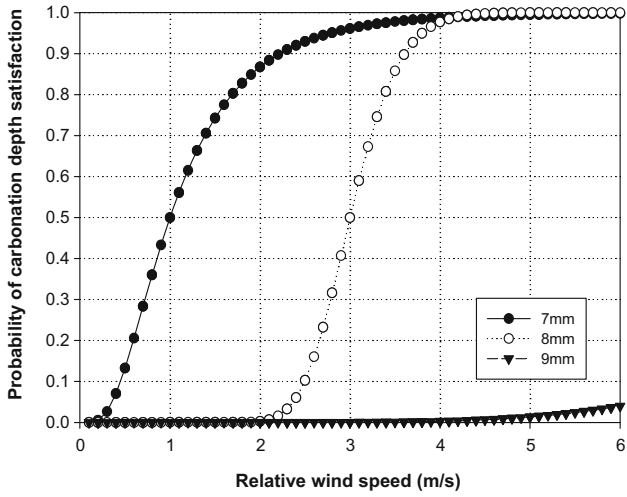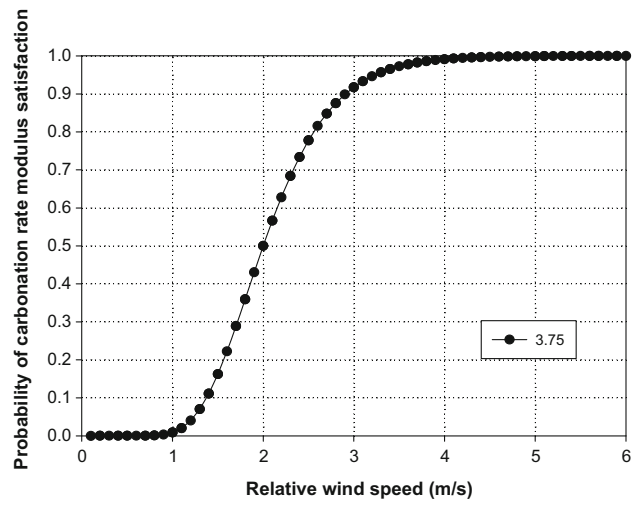
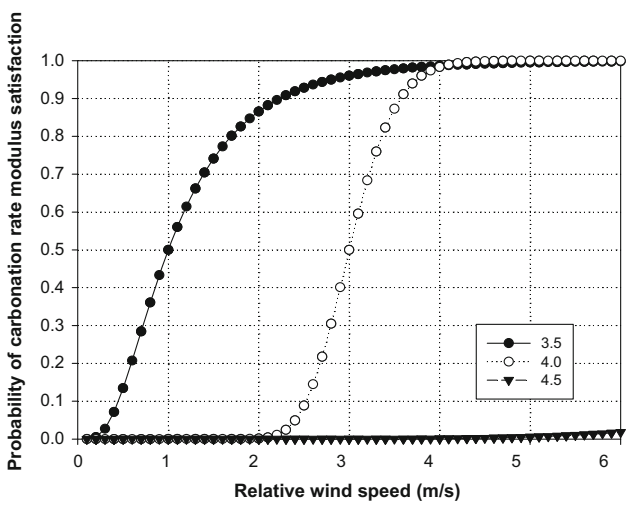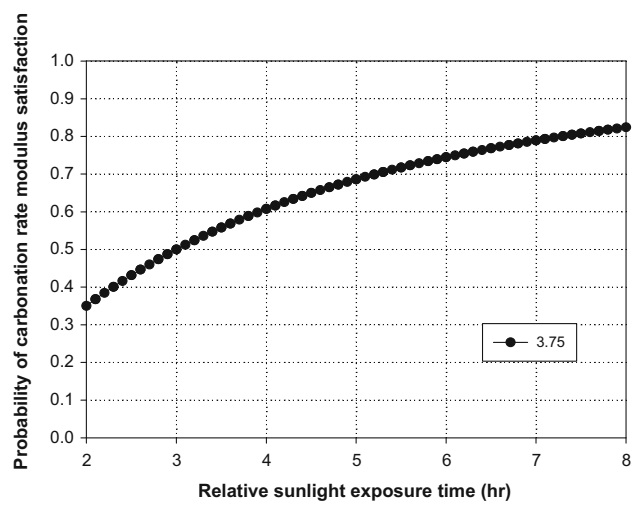**Fig. 6** Satisfaction curve of wind speed parameter for combine carbonation depth (7, 8, 9 mm).
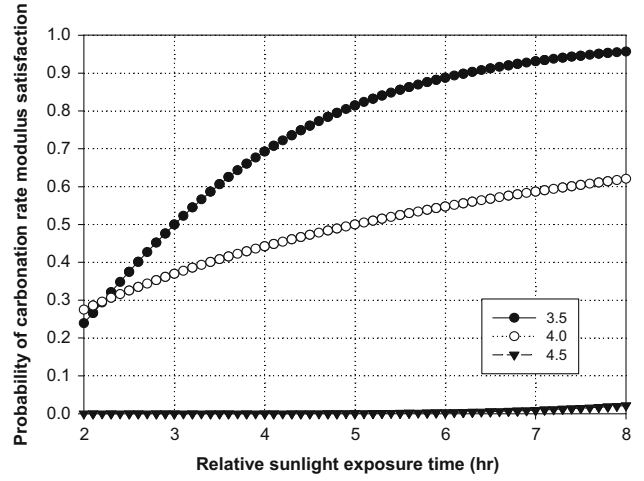
Fig. 7 Satisfaction curve of sunlight exposure time parameter for combine carbonation depth (7, 8, 9 mm).

Fig. 8 Satisfaction curve of wind speed parameter for combine carbonation rate (3.5, 4.0, 4.5).
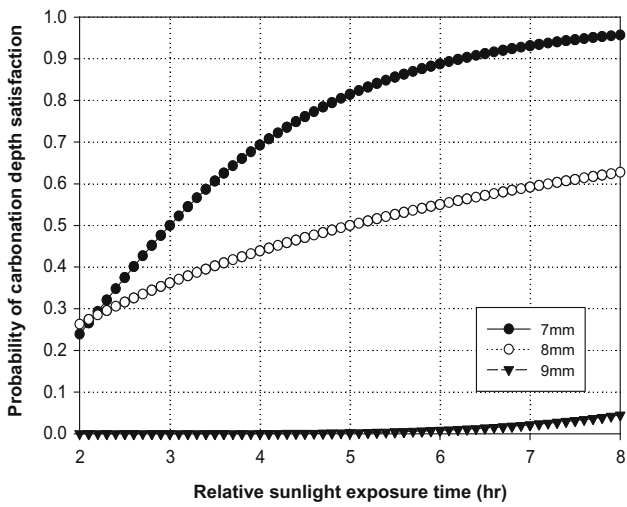
Fig. 9 Satisfaction curve of sunlight exposure time parameter for combine carbonation rate (3.5, 4.0, 4.5).

Fig. 10 Satisfaction Curve of wind speed parameter for carbonation rate (3.75).

Fig. 11 Satisfaction Curve of sunlight exposure time parameter for carbonation rate (3.75).

sunlight exposure time, which suggests that carbonation depth is more affected by wind speed than by sunlight exposure time.

5.2 Satisfaction Curve of Carbonation Rate Modulus

Figures 8 and 9 shows the SCs of carbonation rate modulus as a function of wind speed and sunlight exposure time, and carbonation rate modulus can be set at 3.5, 4, or 4.5, based on Eq. (8). The results, however, show that carbonation rate modulus (3.5, 4, 4.5) is proportional to carbonation depth (7, 8, 9) mm, generating identical SCs. In Fig. 8, for wind speed, 30% and 70% probability satisfaction of designer's required satisfaction specification of 3.5 requires 0.8 and 1.2 m/s curing conditions, respectively. In addition, in Fig. 9, for sunlight exposure time, curing conditions of 2.2 and 4 h are required. In this PBE, various criteria can be set for designer's various required targets, and results of setting required satisfaction criteria by changing carbonation rate modulus to 3.75 are shown in Figs. 10 and 11.

6. Application of Future Climate Scenario

6.1 Result of RCP Scenario Application

Representative Concentration Pathways (RCP) scenarios developed in 2010 year provide four scenarios for how greenhouse gas (GHG) emissions concentration in the atmosphere will be until 2050 year based on factors such as air pollutants and land use change, including RCP 2.6 (the Earth can recover from the impact of human activities), RCP 4.5 (GHG mitigation policies are implemented to a significant extent), RCP 6.0 (GHG mitigation policies are implemented to some extent), and RCP 8.5 (GHG emissions level continues the same as the current level). In the four RCP scenarios, RCP 2.6 is classified as a low GHG emissions scenario, RCP 4.5 and 6.0 are classified as moderate GHG emission scenarios, and RCP 8.5 is classified as a high GHG emissions scenario [http://www.kma.go.kr/](KMA: Korea Meteorological Administration). In this study, RCP 8.5 was applied to the NIMS climate change scenario as shown in Fig. 12 (KMA: Korea Meteorological Administration); this choice was mainly for the following reason. The extreme climate change is primarily caused by GHG, and the main component of GHG is CO_2. Therefore, RCP 8.5 was chosen considering the most extreme climate situation in the future among RCP scenarios. Among RCP scenarios, RCP 8.5 is based on the highest CO_2 emissions and amount in the atmosphere, and is suggested to cause the most extreme climate change in the Korean Peninsula and worldwide in the future. In the NIMS (National Institute of Meteorological Sciences) climate change scenario system, future predictions are possible for the average temperature, relative humidity, precipitation, and wind speed. Therefore, in this study, based on the results of comparative analysis of the projections for 2046–2055 years and the existing data on average wind speed for the last 10 years, the following conclusions were drawn. Regarding sunlight exposure time, scenarios do not

Fig. 12 Application of RCP scenarios.

exist. Therefore, the sunlight exposure time was predicted by applying the inverse of the results obtained by applying the precipitation scenario as the sunlight exposure time refers to the amount of time sunlight is shining on the ground surface without hindrance; therefore, sunlight exposure time is expected to decrease as precipitation increases.

Table 8 shows that the average wind speed is estimated at 2.42 m/s for the last 10 years, 2.62 m/s for 2046–2055, indicating little change during the 50-year period. In Table 9, the average sunlight exposure time was 5.3 h for the last 10 years, 4.74 h for 2046–2055, showing little change in the 50-year period, similarly to wind speed.

6.2 Application of RCP 8.5 Scenario to Carbonation Resistance PBE

Figure 13 shows the SCs that represent the change in wind speed and sunlight exposure time by applying the RCP 8.5 scenario. The changes in satisfaction probabilities were found to be small for carbonation even if the 2050 climate is applied. When the Future Climate RCP 8.5 Scenario was applied, the satisfaction curves showed the following changes. The changes in the wind speed and sunlight-exposure time between the last 10 and 50 years showed an approximately 0.3 m/s increase and 0.56-h decrease, respectively. In addition, the satisfaction curves shifted right and left, respectively, as shown in Fig. 13. The results showed that the satisfaction probabilities for wind speed with threshold carbonation rate modulus of 3.5, 4.0, and 4.5 increased by approximately 5, 20, and 0%, respectively, whereas the satisfaction probabilities for the sunlight-exposure time with the same threshold values decreased by approximately 5, 2, and 0%, respectively. The results suggest that the increase in wind speed and the decrease in sunlight-exposure time lead to increased water evaporation, porosity and lower temperature, which would affect concrete curing process and cause durability degradation. Carbonation penetration rate is

Table 8 Change in wind speed by RCP scenario.

	Wind speed (m/s)	
Period	Past 10 (years)	2046–2055 (years)
Jan.	2.35	2.69
Feb.	2.54	2.99
Mar.	2.83	3.3
Apr.	2.83	3.16
May.	2.5	2.45
Jun.	2.36	2.24
Jul.	2.31	2.48
Aug.	2.34	2.26
Sep.	2.05	2.26
Oct.	2.05	2.38
Nov.	2.37	2.57
Dec.	2.46	2.65

Table 9 Change in sunlight exposure time by RCP scenario.

	Sunlight exposure time (h)	
Period	Past 10 (years)	2046–2055 (years)
Jan.	5.45	3.61
Feb.	5.74	3.94
Mar.	5.81	4.52
Apr.	6.15	3.43
May.	6.48	5.95
Jun.	5.59	4.09
Jul.	2.84	3.21
Aug.	4.01	5.78
Sep.	5.11	12.43
Oct.	6.50	4.06
Nov.	5.06	3.69
Dec.	5.30	2.20
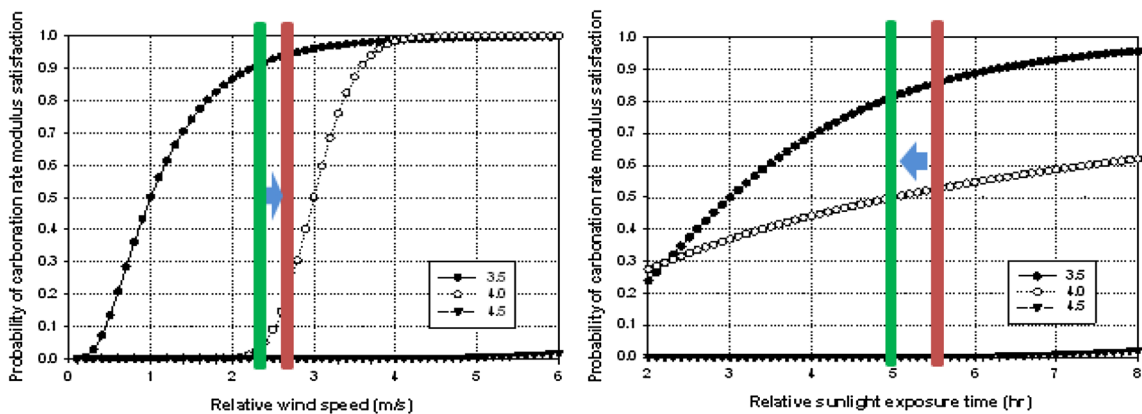
Fig. 13 Application of RCP for climate change scenarios on carbonation speed modulus.

affected by gas permeability, strength, type of cement, mixing condition, and construction condition, in a complex manner. Among them, concrete mixing condition in particular has the greatest effect on carbonation speed, and the carbonation speed increases as W/B increases; therefore, it is efficient to reduce W/B considering carbonation resistance of concrete. Therefore, when W/C is decreased in the mix used in this study considering water tightness, carbonation satisfaction probability will be increased.

6.3 Solutions to the Concrete Carbonation Problem

The following solutions based on literature are proposed to increase concrete carbonation resistance (Khunthongkeaw et al. 2006; Fattuhi 1986; Monteiro et al. 2015). When concrete structures are subject to carbonation, their performance degrades due to the corrosion of reinforcement bars. One method of resisting carbonation is to reduce W/B, which is most influential in mixing, by about 5%, which can reduce carbonation depth by about 30%; another is the use of early-strength Portland cement rather general Portland cement, which can decrease carbonation speed to about 40%. In addition, carbonation resistance can be increased by the application of various coatings for hard concrete, as well as by ensuring a sufficient thickness of concrete in general construction. According to previous studies, nano-composite hybrid-type polymer coating increases carbonation resistance by 90%, and conventional epoxy coating increases carbonation resistance by about 50% (Park 2008; Jung 1992; Choi and Choi 2009, Park et al. 2003).

7. Conclusions

In this study, experimental evaluations were carried out to determine the effects of wind speed, and sunlight exposure time curing conditions from climate change factors on concrete strength and carbonation resistance. Then, SCs were drawn for the performance based evaluation using the Bayesian statistical method. The results obtained in the present study can be summarized as follows.

1. Regarding compressive strength in various wind speed–sunlight exposure time curing conditions, although 3- and 7-day strengths were found to develop normally in all conditions, 28-day long-term strength showed strength degradation in all conditions except 0 m/s wind speed. This performance degradation is thought to have occurred because hydration reaction did not properly occur due to movement of moisture within specimens and water evaluation caused by curing conditions of wind speed and sunlight exposure time.

2. The following conclusion was drawn based on concrete carbonation resistance durability experiments. It was found that in all conditions except a few curing conditions, such as 0 and 2 m/s wind speeds, a considerable level of concrete durability degradation occurs. The prime cause of this phenomenon is thought to be water movement and evaporation during curing with wind speed and sunlight exposure time, which increases porosity in concrete specimens, creates small cracks causing concrete durability degradation.

3. PBE can be conducted based on SCs that are generated with virtual data derived from experimental data obtained from strength and durability experiments using various curing conditions. As PBE allows structure performance evaluation tailored to the designer's various satisfaction requirements, it is thought to be applicable to various construction sites in the future.

4. The results of this study are based on a limited number of curing conditions related to climate change. More varieties of curing conditions and mixing conditions as well as long-term measurements in the durability assessment will be incorporated in future studies.

Acknowledgements

Open Access

References

Al-Khaiat, H., & Fattuhi, N. (2002). Carbonation of concrete exposed to hot and arid climate. *Journal of Materials in Civil Engineering, 14*(2), 97–107.

Ang, A. H. S., & Tang, W. H. (1984). *Probability concept in engineering planning and design*. New York: Wiley.

Box, G. E. P., & Tiao, G. C. (1973). *Bayesian inference in statistical analysis*. New York: Wiley.

Chang, C. F., & Chen, J. W. (2006). The experimental investigation of concrete carbonation depth. *Cement and Concrete Research, 36*(9), 1760–1767.

Choi, D. S., & Choi, J. J. (2009). Experimental study on the time-dependent property of chloride diffusivity of concrete. *Korea Society of Civil Engineers, 29*(4A), 365–371.

Fattuhi, N. I. (1986). Carbonation of concrete as affected by mix constituents and initial water curing period. *Materials and Structures, 19*(2), 131–136.

Fattuhi, N. I. (1988). Concrete carbonation as influenced by curing regime. *Cement and Concrete Research, 18*(3), 426–430.

Jung, J. D. (1992). Present status of researches on carbonation of concrete. *Korea Concrete Institute, 4*(1), 17–24.

Jung, H. J., & Kim, G. S. (2010). A long-term durability prediction for RC structures exposed to carbonation using probabilistic approach. *Korea Institute for Structure Maintenance and Inspection, 14*(5), 119–127.

Kang, W. S. (2004). The impacts and measures of climate change on construction industry. Report of Construction Economy Research Institute. Gangnam, Seoul.

Khunthongkeaw, J., Tangtermsirikul, S., & Leelawat, T. (2006). A study on carbonation depth prediction for fly ash concrete. *Construction and Building Materials, 20*(9), 744–753.

Kim, J. H., Oh, K. C., & Park, S. B. (2008). A study on carbonation velocity for concrete structures. *Korea Institute for Structure Maintenance and Inspection, 12*(2), 163–170.

Kim, J. H. J., Phan, D. H., Kim, B. Y., Choi, J. W., & Han, D. S. (2012). Development of satisfaction curves to evaluate concrete mix design performance using a bayesian probabilistic method. *Construction and Building Materials, 27*(1), 578–584.

Kim, J. H. J., Phan, H. D., Yi, N. H., Kim, S. B., & Jeong, H. S. (2011). Application of the one parameter Bayesian method as the PBMD for concrete mix proportion design. *Magazine of Concrete Research, 63*(1), 31–47.

KS F 2403. (2014). *Standard test method for making and curing concrete specimens*. Korea Standards Association. http://www.kma.go.kr/.

KS F 2584. (2010). *Standard test method for accelerated carbonation of concrete*. Korea Standards Association.

Kwon, S. J., Park, S. S., & Nam, S. H. (2007). A suggestion for carbonation prediction using domestic field survey data of carbonation. *Korea Institute for Structure Maintenance and Inspection, 11*(5), 81–88.

Lo, Y., & Lee, H. M. (2002). Curing effects on carbonation of concrete using a phenolphthalein indicator and Fourier-transform infrared spectroscopy. *Building and Environment, 37*(5), 507–514.

Monteiro, I., Branco, F. A., De Brito, J., & Neves, R. (2015). Statistical analysis of the carbonation coefficient in open air concrete structures. *Construction and Building Materials, 29,* 263–269.

Pachauri, P. K., & Meyer, L.A. (2014). Contribution of working groups I, II and III to the fifth assessment report of the intergovernmental panel on climate change. IPCC, Synthesis Report. Geneva, Switzerland.

Park, D. C. (2008). Carbonation of concrete in relation to CO2 permeability and degradation of coatings. *Construction and Building Materials, 22*(11), 2260–2268.

Park, H. W., Song, H. W., Back, J. M., Woo, J. T., & Nam, J. W. (2003). An experimental study on durability evaluation of nano composite hybrid polymer type coatings applied concrete. *Korea Concrete Institute, 15*(1), 687–692.

Phan, H. D., Kim, J. H. J., Yi, N. H., You, Y. J., & Kim, J. W. (2012). Strength targeted PBMD of HSC based on one-parameter Bayesian probabilistic method. *Advanced Concrete Technology, 10*(4), 137–150.

Shinozuka, M., Feng, M. Q., Kim, H., Uzawa, T., & Ueda, T. (2001). Statistical analysis of fragility curves. Technical Report, Multidisciplinary Center for Earthquake Engineering Research (MCEER), Buffalo, NY, USA.

Shinozuka, M., Feng, M. Q., Lee, J. H., & Naganuma, T. (2000). Statistical analysis of fragility curves. *Journal of Engineering and Mechanic, 126*(12), 1224–1231.

Singhal, A., & Kiremidjian, A. S. (1988). Bayesian updating of fragilities with application to RC frames. *Journal of Structural Engineering, 124*(8), 922–929.

Singhal, A., & Kiremidjian, A. S. (1996). Method for probabilistic evaluation of seismic structural damage. *Journal of Structural Engineering, 122*(12), 1459–1467.

Stoker, T. F., Qin, D., Plattner, G. K., Tignor, M., Allen, S. K., Boschung, J., et al. (2013). The physical science basis. Contributions of working Group I to the fourth assessment report of the intergovernmental panel on climate change. *IPCC*. Cambridge University Press, Cambridge, United Kingdom and New York, NY